Perturbation theory of quantum dot attached to two superconducting leads

Martin Žonda, Vladislav Pokorný, Václav Janiš, Tomáš Novotný

Department of Condensed Matter Physics, FMP, Charles University and Institute of Physics, CAS

Vietri sul Mare 2016

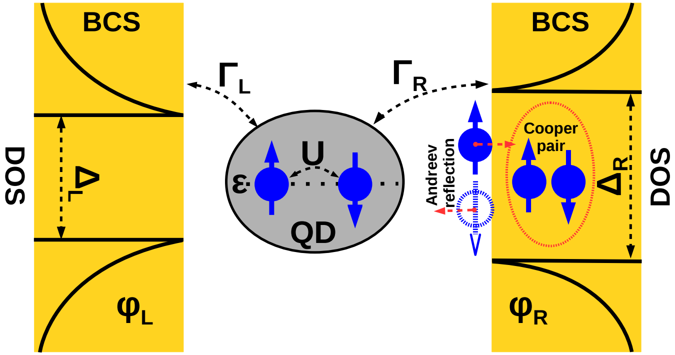
BCS
BCS
Γ_L
Γ_R
DOS
Δ_L
ε
U
QD
Andreev reflection
Cooper pair
Δ_R
DOS
φ_L
φ_R

1. Introduction
    - Single Impurity Anderson Model
2. Methods
    - Green function
    - Spin-symmetric Hartree-Fock approximation
    - Dynamical corrections
3. Discussion
    - ABS and supercurrent
    - Phase diagrams
    - Comparison with experiments
4. Conclusions

Superconducting Quantum Dot

There are many experimental realizations of a single-level quantum dot connected to BCS leads, e.g.:

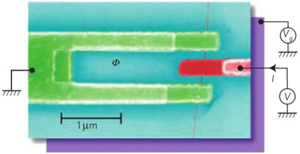

CNT
Nat. Phys. 6, 965 (2010)

Superconducting Quantum Dot

There are many experimental realizations of a single-level quantum dot connected to BCS leads, e.g.:

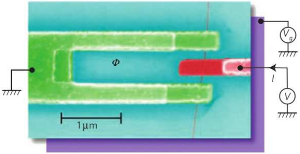

CNT
Nat. Phys. 6, 965 (2010)

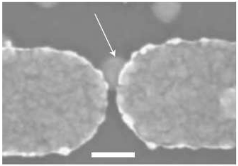

SiGe
Nat. Nano. 5, 458 (2010)

Superconducting Quantum Dot

There are many experimental realizations of a single-level quantum dot connected to BCS leads, e.g.:

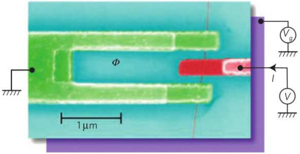

CNT
Nat. Phys. 6, 965 (2010)

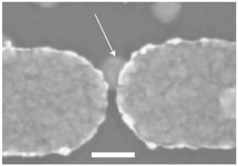

SiGe
Nat. Nano. 5, 458 (2010)

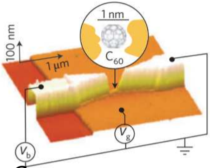

C_{60}
Nat. 453, 633 (2008)

Superconducting Quantum Dot

There are many experimental realizations of a single-level quantum dot connected to BCS leads, e.g.:

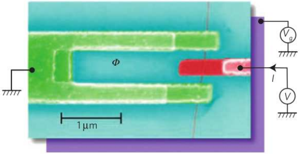

CNT
Nat. Phys. 6, 965 (2010)

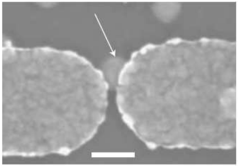

SiGe
Nat. Nano. 5, 458 (2010)

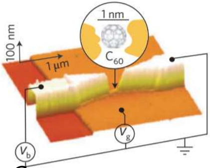

C_{60}
Nat. 453, 633 (2008)

- These devices are generalized Josephson junctions!

Superconducting Quantum Dot

There are many experimental realizations of a single-level quantum dot connected to BCS leads, e.g.:

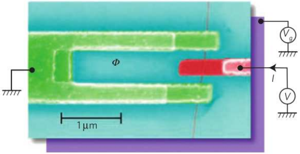

CNT
Nat. Phys. 6, 965 (2010)

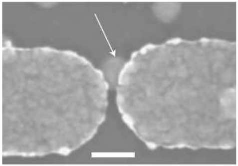

SiGe
Nat. Nano. 5, 458 (2010)

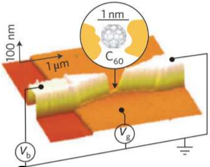

C_{60}
Nat. 453, 633 (2008)

- These devices are generalized Josephson junctions!
- They allow to explore a wide range of phenomena, including electron transport, Kondo physics, quantum entanglement, different quasiparticles or **siglet-doublet phase transition**

SIAM with superconducting leads

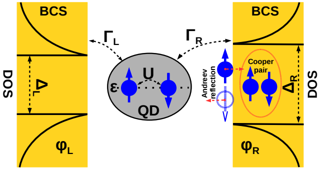

SIAM with superconducting leads

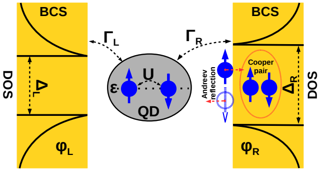

- General impurity hamiltonian:

$$H = H_{imp} + \sum_{\alpha=L,R} H^{\alpha}_{lead} + H^{\alpha}_{hyb}$$

SIAM with superconducting leads

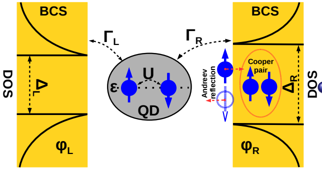

- General impurity hamiltonian:

$$H = H_{imp} + \sum_{\alpha=L,R} H^{\alpha}_{lead} + H^{\alpha}_{hyb}$$

- Single impurity Anderson model (SIAM):

$$H_{imp} = \varepsilon \sum_{\sigma=\uparrow,\downarrow} d^{\dagger}_{\sigma} d_{\sigma} + U\, d^{\dagger}_{\uparrow} d_{\uparrow} d^{\dagger}_{\downarrow} d_{\downarrow},$$

$$H^{\alpha}_{lead} = \sum_{k\sigma} \epsilon_k c^{\dagger}_{\alpha k\sigma} c_{\alpha k\sigma} - \Delta_{\alpha} \sum_{k} e^{i\phi_{\alpha}} c^{\dagger}_{\alpha k\uparrow} c^{\dagger}_{\alpha -k\downarrow} + H.c.$$

$$H^{\alpha}_{hyb} = t_{\alpha} \sum_{k\sigma} \left(d^{\dagger}_{\sigma} c_{\alpha k\sigma} + c^{\dagger}_{\alpha k\sigma} d_{\sigma} \right)$$

SIAM with superconducting leads

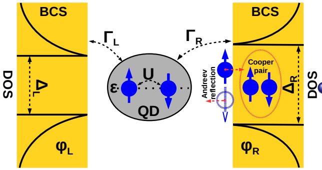

- General impurity hamiltonian:

$$H = H_{imp} + \sum_{\alpha=L,R} H^{\alpha}_{lead} + H^{\alpha}_{hyb}$$

- Single impurity Anderson model (SIAM):

$$H_{imp} = \varepsilon \sum_{\sigma=\uparrow,\downarrow} d^{\dagger}_{\sigma} d_{\sigma} + U\, d^{\dagger}_{\uparrow} d_{\uparrow} d^{\dagger}_{\downarrow} d_{\downarrow},$$

$$H^{\alpha}_{lead} = \sum_{k\sigma} \epsilon_k c^{\dagger}_{\alpha k\sigma} c_{\alpha k\sigma} - \Delta_{\alpha} \sum_{k} e^{i\phi_{\alpha}} c^{\dagger}_{\alpha k\uparrow} c^{\dagger}_{\alpha -k\downarrow} + H.c.$$

$$H^{\alpha}_{hyb} = t_{\alpha} \sum_{k\sigma} \left(d^{\dagger}_{\sigma} c_{\alpha k\sigma} + c^{\dagger}_{\alpha k\sigma} d_{\sigma} \right)$$

- Normal-state tunnel coupling magnitude (energy-independent hybridization): $\Gamma_{\alpha} = \pi t^2_{\alpha} \rho_0$

Basic phase diagram

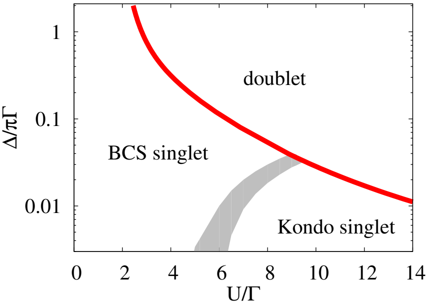

Basic phase diagram

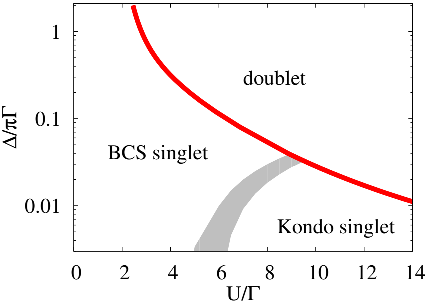

- **BCS singlet**: Singlet with large proximity induced gap $\Delta_d = U \left\langle d_\uparrow^\dagger d_\downarrow^\dagger \right\rangle$

Basic phase diagram

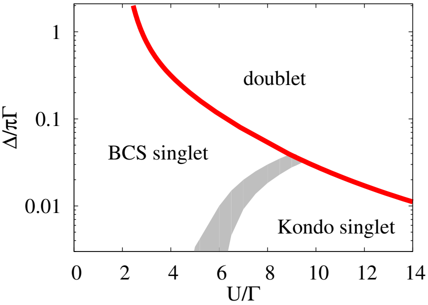

- **BCS singlet**: Singlet with large proximity induced gap $\Delta_d = U \left\langle d_\uparrow^\dagger d_\downarrow^\dagger \right\rangle$
- **Kondo singlet**: The dot is occupied by a single electron whose spin is screened (Kondo screening) by the contribution from band states

Basic phase diagram

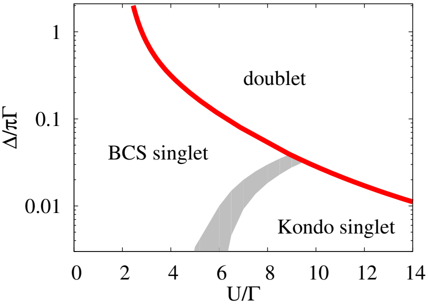

- **BCS singlet**: Singlet with large proximity induced gap $\Delta_d = U \left\langle d_\uparrow^\dagger d_\downarrow^\dagger \right\rangle$
- **Kondo singlet**: The dot is occupied by a single electron whose spin is screened (Kondo screening) by the contribution from band states
- **Doublet**: Spin-doublet with a single electron **degenerate** state

Basic phase diagram

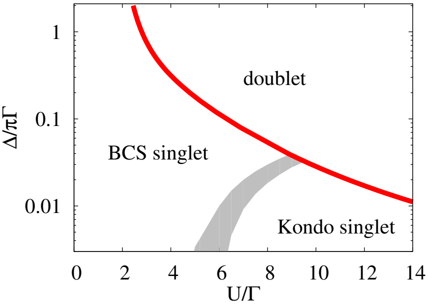

- **BCS singlet**: Singlet with large proximity induced gap $\Delta_d = U \left\langle d^\dagger_\uparrow d^\dagger_\downarrow \right\rangle$
- **Kondo singlet**: The dot is occupied by a single electron whose spin is screened (Kondo screening) by the contribution from band states
- **Doublet**: Spin-doublet with a single electron **degenerate** state

- The $0 - \pi$ transition is induced by the underlying impurity QPT related to the crossing of the lowest many-body eigenstates from a spin-singlet ground state with positive supercurrent (0 phase) to a spin-doublet state with negative supercurrent (π phase)
- This transition is associated with crossing of the Andreev bound states (ABS) at the Fermi energy

Andreev Bound States (ABS)

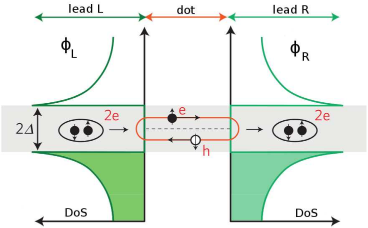

Nat. Phys. 6, 965 (2010)

Andreev Bound States (ABS)

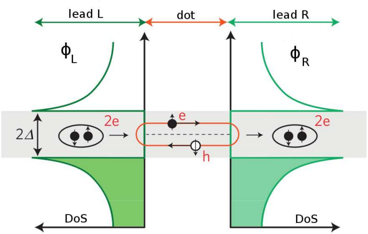

Nat. Phys. 6, 965 (2010)

- Because of the superconducting pairing the electron in the dot with $En. < \Delta$ is reflected as a hole: Andreev reflection

Andreev Bound States (ABS)

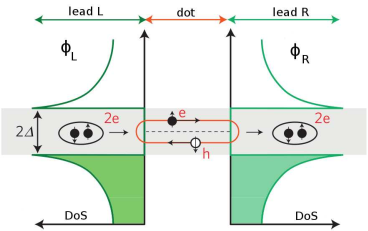

Nat. Phys. 6, 965 (2010)

- Because of the superconducting pairing the electron in the dot with $En. < \Delta$ is reflected as a hole: Andreev reflection
- Analogously the hole is reflected as an electron

Andreev Bound States (ABS)

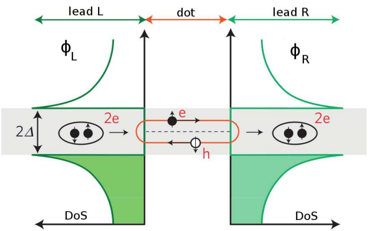

Nat. Phys. 6, 965 (2010)

- Because of the superconducting pairing the electron in the dot with *En.* $< \Delta$ is reflected as a hole: Andreev reflection
- Analogously the hole is reflected as an electron
- As a result of multiple Andreev reflections the resonant standing waves (ABS) with discrete energies $\pm\omega_0$ appear within the superconducting gap

Andreev Bound States (ABS)

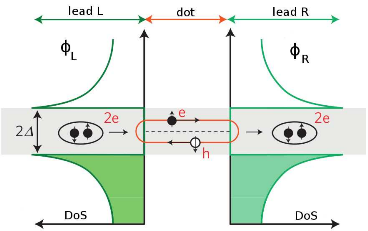

Nat. Phys. 6, 965 (2010)

- Because of the superconducting pairing the electron in the dot with $En. < \Delta$ is reflected as a hole: Andreev reflection
- Analogously the hole is reflected as an electron
- As a result of multiple Andreev reflections the resonant standing waves (ABS) with discrete energies $\pm\omega_0$ appear within the superconducting gap
- Smooth crossing of ABS is associated with the $0 - \pi$ transition induced by impurity quantum phase transition (QMC, NRG, experiments)

Andreev Bound States (ABS)

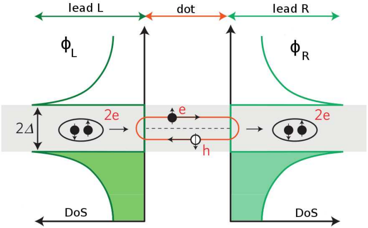

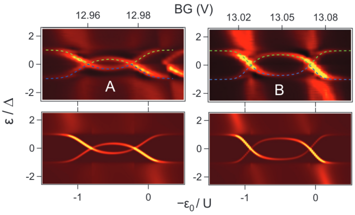

Pillet et. al PRB 88, 045101 (2013)

- Because of the superconducting pairing the electron in the dot with $En. < \Delta$ is reflected as a hole: Andreev reflection
- Analogously the hole is reflected as an electron
- As a result of multiple Andreev reflections the resonant standing waves (ABS) with discrete energies $\pm\omega_0$ appear within the superconducting gap
- Smooth crossing of ABS is associated with the $0 - \pi$ transition induced by impurity quantum phase transition (QMC, NRG, experiments)

Green function

We consider only the **spin-symmetric** solution and $e = \hbar = 1$.

Green function

We consider only the **spin-symmetric** solution and $e = \hbar = 1$.

The exact form of the unperturbed impurity GF ($U = 0$) can be written in the terms of Matsubara frequencies $\omega_n \equiv (2n+1)\pi/\beta$ as:

$$\widehat{G}_0(i\omega_n) = \begin{pmatrix} i\omega_n[1 + s(i\omega_n)] - \varepsilon \ , & \Delta_\Phi(i\omega_n) \\ \Delta^*_\Phi(i\omega_n) \ , & i\omega_n[1 + s(i\omega_n)] + \varepsilon \end{pmatrix}^{-1} ,$$

Green function

We consider only the **spin-symmetric** solution and $e = \hbar = 1$.

The exact form of the unperturbed impurity GF ($U = 0$) can be written in the terms of Matsubara frequencies $\omega_n \equiv (2n+1)\pi/\beta$ as:

$$\widehat{G}_0(i\omega_n) = \begin{pmatrix} i\omega_n[1+s(i\omega_n)] - \varepsilon \ , & \Delta_\Phi(i\omega_n) \\ \Delta^*_\Phi(i\omega_n) \ , & i\omega_n[1+s(i\omega_n)] + \varepsilon \end{pmatrix}^{-1},$$

where $s(i\omega_n) = \sum_{\alpha=L,R} \frac{\Gamma_\alpha}{\sqrt{\Delta_\alpha^2+\omega_n^2}}$ and $\Delta_\Phi(i\omega_n) = \sum_{\alpha=L,R} \frac{\Gamma_\alpha \Delta_\alpha}{\sqrt{\Delta_\alpha^2+\omega_n^2}} e^{i\Phi_\alpha}$

Green function

- Self-energy (SE) matrix:

$$\widehat{\Sigma}(i\omega_n) \equiv \begin{pmatrix} \Sigma(i\omega_n), & \mathcal{S}(i\omega_n) \\ \bar{\mathcal{S}}(i\omega_n), & \bar{\Sigma}(i\omega_n) \end{pmatrix}$$

Green function

- Self-energy (SE) matrix:

$$\widehat{\Sigma}(i\omega_n) \equiv \begin{pmatrix} \Sigma(i\omega_n), & \mathcal{S}(i\omega_n) \\ \bar{\mathcal{S}}(i\omega_n), & \bar{\Sigma}(i\omega_n) \end{pmatrix}$$

- Symmetry relations:

$$\bar{\Sigma}_\sigma(i\omega_n) = -\Sigma_\sigma(-i\omega_n);$$
$$\bar{S}_\sigma(i\omega_n) = S^*_\sigma(-i\omega_n).$$

Green function

- Self-energy (SE) matrix:

$$\widehat{\Sigma}(i\omega_n) \equiv \begin{pmatrix} \Sigma(i\omega_n), & \mathcal{S}(i\omega_n) \\ \bar{\mathcal{S}}(i\omega_n), & \bar{\Sigma}(i\omega_n) \end{pmatrix}$$

- Symmetry relations:

$$\bar{\Sigma}_\sigma(i\omega_n) = -\Sigma_\sigma(-i\omega_n);$$
$$\bar{S}_\sigma(i\omega_n) = S^*_\sigma(-i\omega_n).$$

The interacting Green function reads explicitly:

$$\widehat{G}(i\omega_n) = -\frac{1}{D(i\omega_n)} \begin{pmatrix} i\omega_n[1+s(i\omega_n)] + \varepsilon + \Sigma(-i\omega_n), & -\Delta_\Phi(i\omega_n) + \mathcal{S}(i\omega_n) \\ -\Delta^*_\Phi(i\omega_n) + \mathcal{S}^*(-i\omega_n), & i\omega_n[1+s(i\omega_n)] - \varepsilon - \Sigma(i\omega_n) \end{pmatrix}$$

Green function

- Self-energy (SE) matrix:

$$\widehat{\Sigma}(i\omega_n) \equiv \begin{pmatrix} \Sigma(i\omega_n), & \mathcal{S}(i\omega_n) \\ \bar{\mathcal{S}}(i\omega_n), & \bar{\Sigma}(i\omega_n) \end{pmatrix}$$

- Symmetry relations:

$$\bar{\Sigma}_\sigma(i\omega_n) = -\Sigma_\sigma(-i\omega_n); \quad \bar{S}_\sigma(i\omega_n) = S^*_\sigma(-i\omega_n).$$

The interacting Green function reads explicitly:

$$\widehat{G}(i\omega_n) = -\frac{1}{D(i\omega_n)} \begin{pmatrix} i\omega_n[1+s(i\omega_n)] + \varepsilon + \Sigma(-i\omega_n), & -\Delta_\Phi(i\omega_n) + \mathcal{S}(i\omega_n) \\ -\Delta^*_\Phi(i\omega_n) + \mathcal{S}^*(-i\omega_n), & i\omega_n[1+s(i\omega_n)] - \varepsilon - \Sigma(i\omega_n) \end{pmatrix}$$

ABS are determined by the zeros of the determinant (poles of $\widehat{G}(i\omega_n)$) :

$$\begin{aligned} D(i\omega_n) = \; & \omega_n^2 \left[1 + s(i\omega_n)\right]^2 + \left[\varepsilon + \Sigma(i\omega_n)\right]\left[\varepsilon + \Sigma(-i\omega_n)\right] \\ & + \left[\Delta_\Phi(i\omega_n) - \mathcal{S}(i\omega_n)\right]\left[\Delta^*_\Phi(i\omega_n) - \mathcal{S}^*(-i\omega_n)\right] \end{aligned}$$

Spin-symmetric Hartree-Fock

Spin-symmetric Hartree-Fock

- The first order Hartree-Fock contributions to the self-energies read:

Spin-symmetric Hartree-Fock

- The first order Hartree-Fock contributions to the self-energies read:
  $\Sigma^{HF} = \frac{U}{\beta} \sum_{n\in\mathbb{Z}} G(i\omega_n) e^{i\omega_n 0^+}$ and $\mathcal{S}^{HF} = \frac{U}{\beta} \sum_{n\in\mathbb{Z}} \mathcal{G}(i\omega_n)$

Spin-symmetric Hartree-Fock

- The first order Hartree-Fock contributions to the self-energies read: $\Sigma^{HF} = \frac{U}{\beta}\sum_{n\in\mathbb{Z}} G(i\omega_n)e^{i\omega_n 0^+}$ and $\mathcal{S}^{HF} = \frac{U}{\beta}\sum_{n\in\mathbb{Z}} \mathcal{G}(i\omega_n)$
- Despite its simplicity (and contrary to the common belief), HF yields the $0-\pi$ phase transition without spin-symmetry breaking.

Spin-symmetric Hartree-Fock

- The first order Hartree-Fock contributions to the self-energies read: $\Sigma^{HF} = \frac{U}{\beta}\sum_{n\in\mathbb{Z}} G(i\omega_n)e^{i\omega_n 0^+}$ and $\mathcal{S}^{HF} = \frac{U}{\beta}\sum_{n\in\mathbb{Z}} \mathcal{G}(i\omega_n)$
- Despite its simplicity (and contrary to the common belief), HF yields the $0-\pi$ phase transition without spin-symmetry breaking.
- Moreover, the HF phase boundary can be found analytically:

$$\left[\frac{U}{2\left(1+\frac{\Gamma_L}{\Delta_L}+\frac{\Gamma_R}{\Delta_R}\right)}\right] = \left[\varepsilon+\frac{U}{2}\right]^2 + \left[(\Gamma_L-\Gamma_R)^2 + 4\Gamma_L\Gamma_R\cos^2\frac{\Phi}{2}\right][1+U\mathcal{B}]^2$$

Spin-symmetric Hartree-Fock

- The first order Hartree-Fock contributions to the self-energies read:
  $\Sigma^{HF} = \frac{U}{\beta}\sum_{n\in\mathbb{Z}} G(i\omega_n)e^{i\omega_n 0^+}$ and $\mathcal{S}^{HF} = \frac{U}{\beta}\sum_{n\in\mathbb{Z}} \mathcal{G}(i\omega_n)$
- Despite its simplicity (and contrary to the common belief), HF yields the $0-\pi$ phase transition without spin-symmetry breaking.
- Moreover, the HF phase boundary can be found analytically:

$$\left[\frac{U}{2\left(1+\frac{\Gamma_L}{\Delta_L}+\frac{\Gamma_R}{\Delta_R}\right)}\right] = \left[\varepsilon+\frac{U}{2}\right]^2 + \left[(\Gamma_L-\Gamma_R)^2 + 4\Gamma_L\Gamma_R\cos^2\frac{\Phi}{2}\right][1+U\mathcal{B}]^2$$

- Where $\mathcal{B}$ is the band contribution:

$$\mathcal{B} = \int_0^\infty \frac{d\omega}{\pi}\frac{\sum\limits_\alpha \Gamma_\alpha e^{i\Phi_\alpha}\left(1-\frac{\Delta_\alpha}{\sqrt{\Delta_\alpha^2+\omega^2}}\right)}{\omega^2\left[1+\sum_\alpha \frac{\Gamma_\alpha}{\sqrt{\Delta_\alpha^2+\omega^2}}\right]^2 + \left|\sum_\alpha \Gamma_\alpha e^{i\Phi_\alpha}\left(\frac{\Delta_\alpha}{\sqrt{\Delta_\alpha^2+\omega^2}}-1\right)\right|^2}$$

Spin-symmetric Hartree-Fock

- The first order Hartree-Fock contributions to the self-energies read: $\Sigma^{HF} = \frac{U}{\beta}\sum_{n\in\mathbb{Z}} G(i\omega_n)e^{i\omega_n 0^+}$ and $\mathcal{S}^{HF} = \frac{U}{\beta}\sum_{n\in\mathbb{Z}} \mathcal{G}(i\omega_n)$
- Despite its simplicity (and contrary to the common belief), HF yields the $0-\pi$ phase transition without spin-symmetry breaking.
- Moreover, the HF phase boundary can be found analytically:

$$\left[\frac{U}{2\left(1+\frac{\Gamma_L}{\Delta_L}+\frac{\Gamma_R}{\Delta_R}\right)}\right] = \left[\varepsilon + \frac{U}{2}\right]^2 + \left[(\Gamma_L-\Gamma_R)^2 + 4\Gamma_L\Gamma_R\cos^2\frac{\Phi}{2}\right][1+U\mathcal{B}]^2$$

- By omitting the band contribution $\mathcal{B}=0$ one gets an extremely simple (and often surprisingly good) approximation: **generalized atomic limit** (GAL)

Dynamical corrections

- The HF approximation leads only to static, frequency-independent mean-field SE. This is not enough for the quantitative predictions!

Dynamical corrections

- The HF approximation leads only to static, frequency-independent mean-field SE. This is not enough for the quantitative predictions!
- The simplest dynamical corrections come from the second order of the perturbation expansion:

Dynamical corrections

- The HF approximation leads only to static, frequency-independent mean-field SE. This is not enough for the quantitative predictions!
- The simplest dynamical corrections come from the second order of the perturbation expansion:

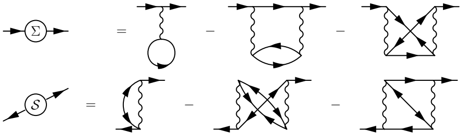

Dynamical corrections

- The HF approximation leads only to static, frequency-independent mean-field SE. This is not enough for the quantitative predictions!
- The simplest dynamical corrections come from the second order of the perturbation expansion:

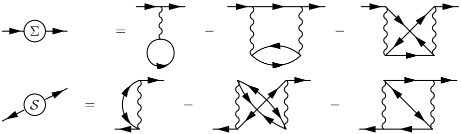

- With the mathematical equivalents:

$$\Sigma^{(2)}(i\omega_n) = -\frac{U^2}{\beta}\sum_{m\in\mathbb{Z}} G(i\omega_n + i\nu_m)\chi(i\nu_m),\ \mathcal{S}^{(2)}(i\omega_n) = -\frac{U^2}{\beta}\sum_{m\in\mathbb{Z}} \mathcal{G}(i\omega_n + i\nu_m)\chi(i\nu_m),$$

Dynamical corrections

- The HF approximation leads only to static, frequency-independent mean-field SE. This is not enough for the quantitative predictions!
- The simplest dynamical corrections come from the second order of the perturbation expansion:

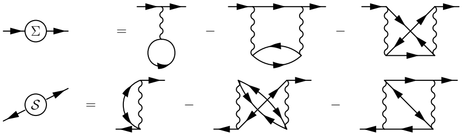

- With the mathematical equivalents:

$$\Sigma^{(2)}(i\omega_n) = -\frac{U^2}{\beta}\sum_{m\in\mathbb{Z}} G(i\omega_n + i\nu_m)\chi(i\nu_m),\ \mathcal{S}^{(2)}(i\omega_n) = -\frac{U^2}{\beta}\sum_{m\in\mathbb{Z}} \mathcal{G}(i\omega_n + i\nu_m)\chi(i\nu_m),$$

where the two-particle bubble consists of normal and anomalous parts:

$$\chi(i\nu_m) = \frac{1}{\beta}\sum \left[G(i\omega_n)G(i\omega_n + i\nu_m) + \mathcal{G}(i\omega_n)\mathcal{G}(i\omega_n + i\nu_m)\right]$$

Dynamical corrections

- The HF approximation leads only to static, frequency-independent mean-field SE. This is not enough for the quantitative predictions!
- The simplest dynamical corrections come from the second order of the perturbation expansion:

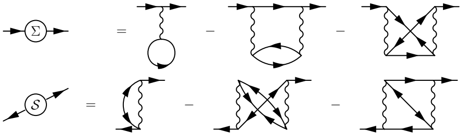

- Self-consistent solution
  - full self-consistent dynamical correction (FDC) approximation
  - evaluating the dynamical self-energies using just a fully converged HF solution as the input into GF (DC)

DC vs FDC vs NRG

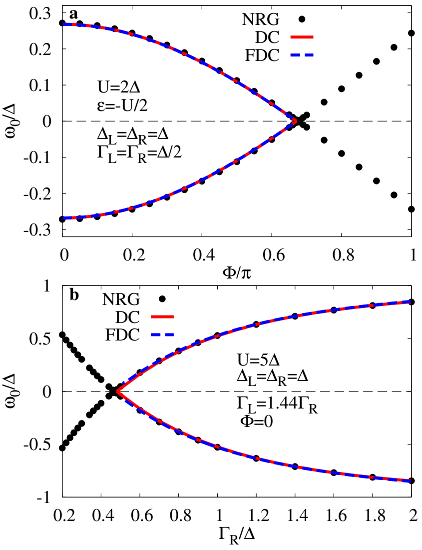

DC vs FDC vs NRG

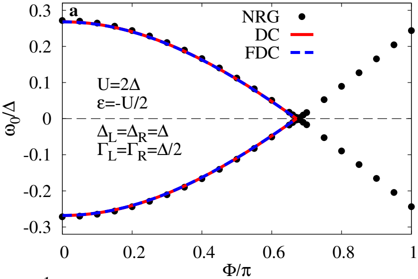

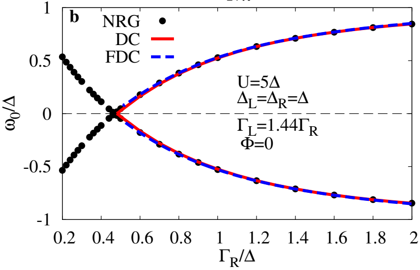

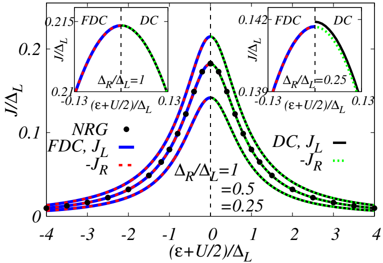

DC vs FDC vs NRG

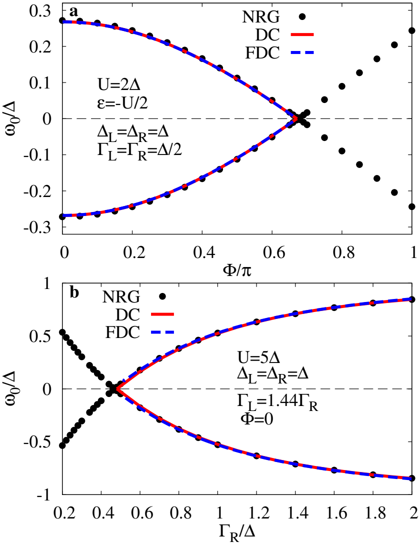

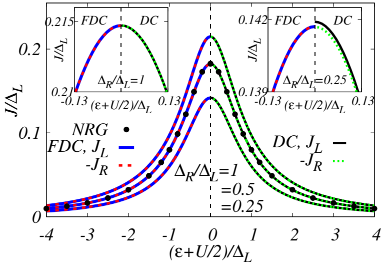

- FDC is charge conserving in the general case

DC vs FDC vs NRG

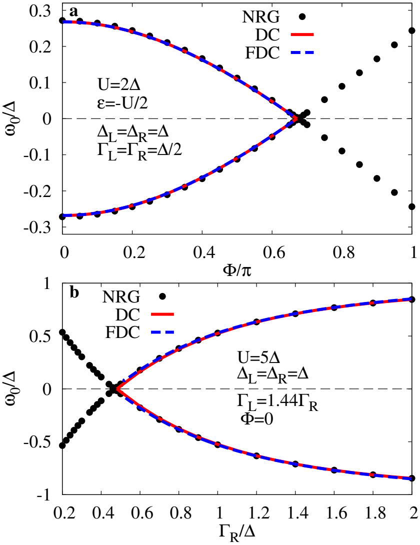

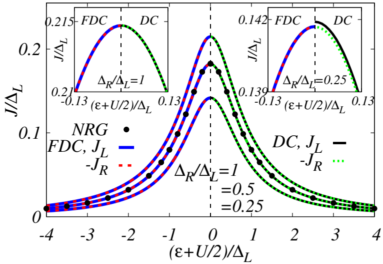

- FDC is charge conserving in the general case
- DC is charge conserving for equal gaps

DC vs FDC vs NRG

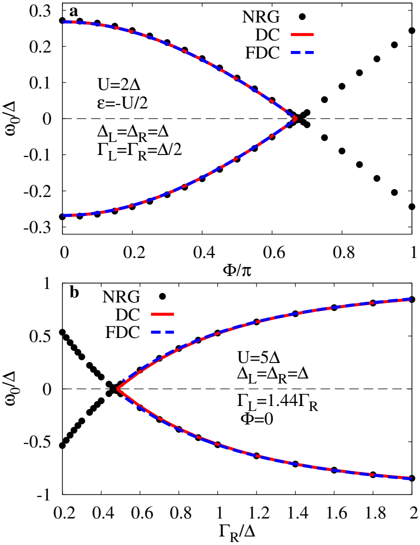

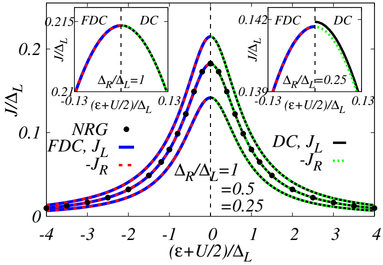

- FDC is charge conserving in the general case
- DC is charge conserving for equal gaps
- - proven analytically in M.Ž. et. al, PRB 93, 024523 (2016)

Phase diagrams: $\Gamma_L = \Gamma_R = \Gamma/2$,$\Delta_L = \Delta_R$, half-filling

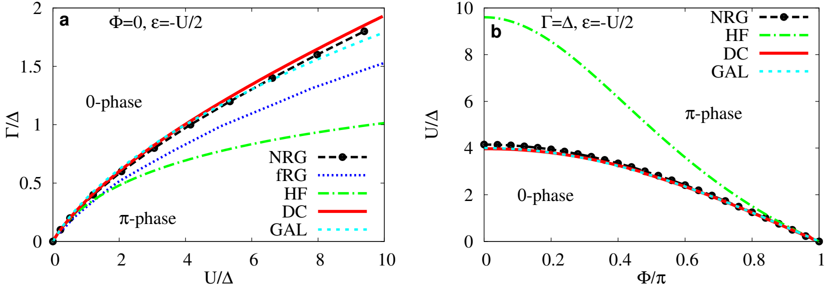

(fRG data taken from Karrasch, PRB (2008))

Phase diagrams: $\Gamma_L = \Gamma_R = \Gamma/2$,$\Delta_L = \Delta_R$, half-filling

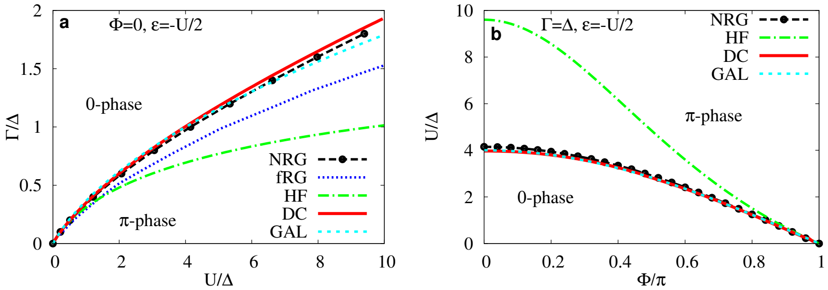

(fRG data taken from Karrasch, PRB (2008))

- **DC** and **GAL** are in surprisingly good agreement with NRG

Phase diagrams: $\Gamma_L = \Gamma_R = \Gamma/2$,$\Delta_L = \Delta_R$, half-filling

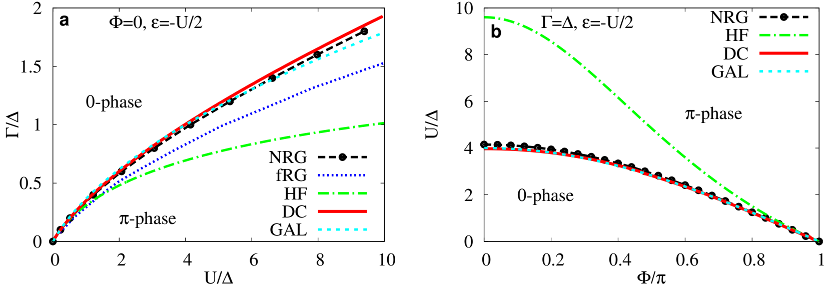

(fRG data taken from Karrasch, PRB (2008))

- **DC** and **GAL** are in surprisingly good agreement with NRG
- **HF** overestimates the contribution from the bands

Phase diagrams: $\Gamma_L \neq \Gamma_R$, $\Delta_L = \Delta_R$

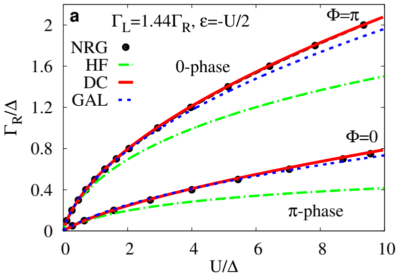

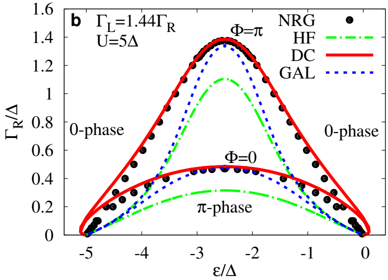

Phase diagrams: $\Gamma_L \neq \Gamma_R$, $\Delta_L = \Delta_R$

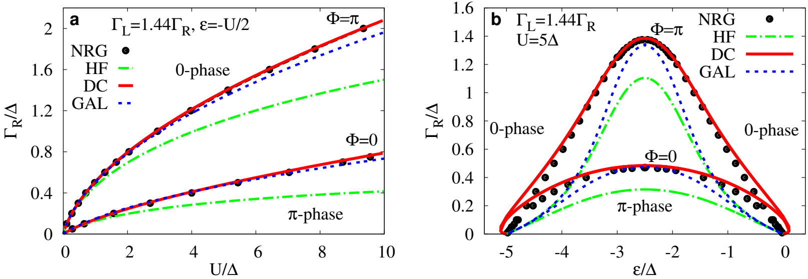

- GAL provides a very good and fast approximation of the phase boundary at **half-filling** even for $U \gg \Delta$

Phase diagrams: $\Gamma_L \neq \Gamma_R$, $\Delta_L = \Delta_R$

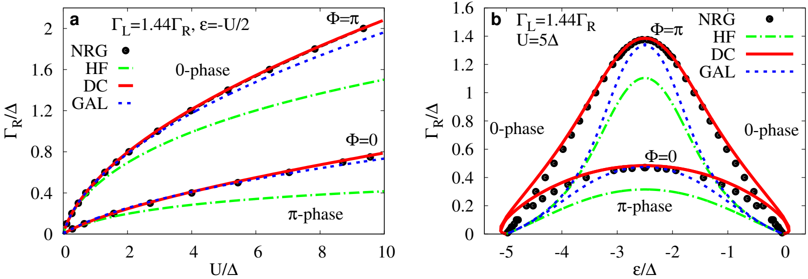

- GAL provides a very good and fast approximation of the phase boundary at **half-filling** even for $U \gg \Delta$
- For $U \gg \Gamma$ we enter the Kondo regime, therefore the discrepancy between NRG nad DC

Grenoble experiment [Phys. Rev. X 2, 011009 (2012)]

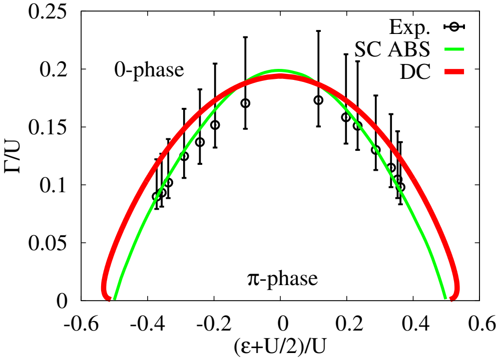

Grenoble experiment [Phys. Rev. X 2, 011009 (2012)]

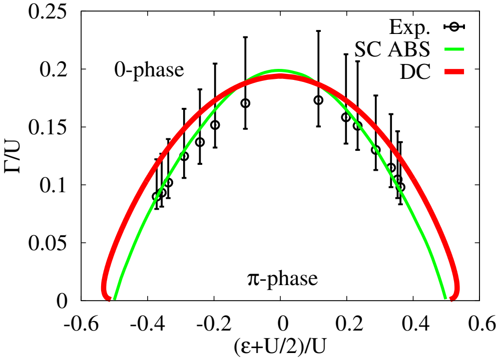

- Realization of a fully tunable superconducting CNT quantum dot SQUID by Maurand et al.

Grenoble experiment [Phys. Rev. X 2, 011009 (2012)]

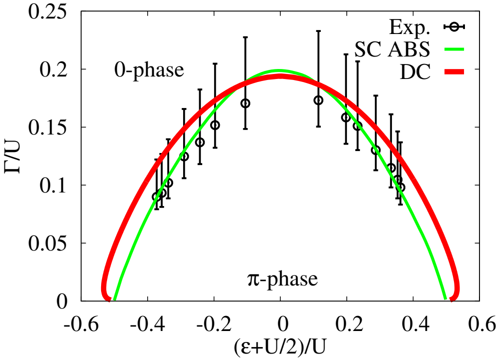

- Realization of a fully tunable superconducting CNT quantum dot SQUID by Maurand et al.
- The tunneling amplitudes to the leads were balanced $\Gamma/2 = \Gamma_L = \Gamma_R$

Grenoble experiment [Phys. Rev. X 2, 011009 (2012)]

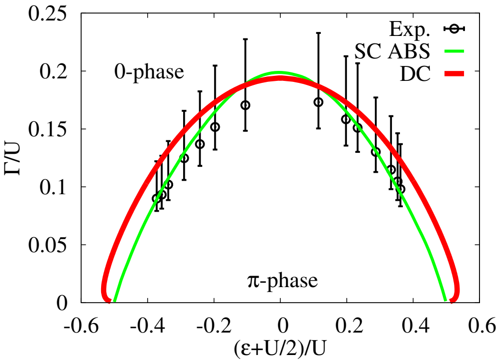

- Realization of a fully tunable superconducting CNT quantum dot SQUID by Maurand et al.
- The tunneling amplitudes to the leads were balanced $\Gamma/2 = \Gamma_L = \Gamma_R$
- The authors argue that the Kondo screening plays a key role for the phase transition in their device ($U \simeq 0.8$ meV and SC $\Delta \simeq 0.08$ meV)

Grenoble experiment [Phys. Rev. X 2, 011009 (2012)]

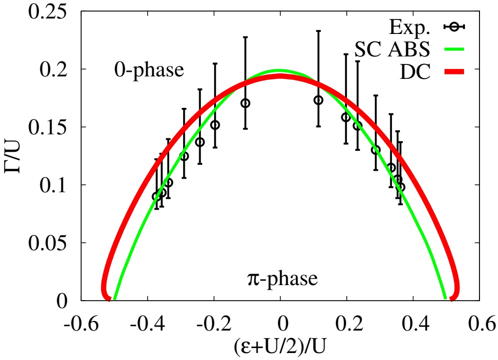

- Realization of a fully tunable superconducting CNT quantum dot SQUID by Maurand et al.
- The tunneling amplitudes to the leads were balanced $\Gamma/2 = \Gamma_L = \Gamma_R$
- The authors argue that the Kondo screening plays a key role for the phase transition in their device ($U \simeq 0.8$ meV and SC $\Delta \simeq 0.08$ meV)
- The SC ABS ($U = 10\Delta$) is very close to the experimental data

Grenoble experiment [Phys. Rev. X 2, 011009 (2012)]

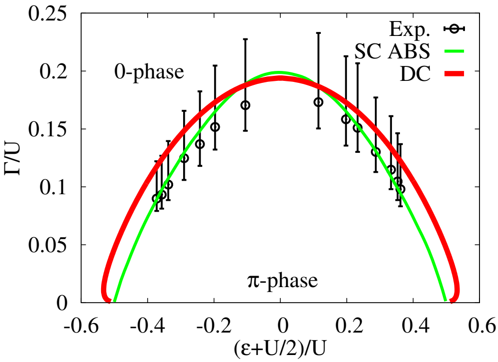

- Realization of a fully tunable superconducting CNT quantum dot SQUID by Maurand et al.
- The tunneling amplitudes to the leads were balanced $\Gamma/2 = \Gamma_L = \Gamma_R$
- The authors argue that the Kondo screening plays a key role for the phase transition in their device ($U \simeq 0.8$ meV and SC $\Delta \simeq 0.08$ meV)
- The SC ABS ($U = 10\Delta$) is very close to the experimental data
- DC performs well even beyond its expected validity

Orsay experiment [Phys. Rev. B 91, 241401(R) (2015)]

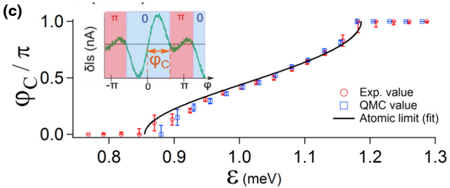

R. Delagrange et. al Phys. Rev. B 91, 241401(R) (2015)

Orsay experiment [Phys. Rev. B 91, 241401(R) (2015)]

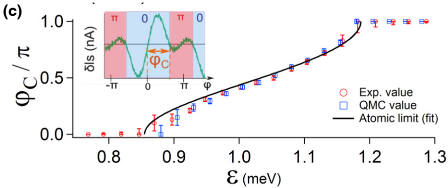

R. Delagrange et. al Phys. Rev. B 91, 241401(R) (2015)

- Experimental confirmation of the $0-\pi$ transition controlled by the gate voltage in CNT by Delagrange et al.

Orsay experiment [Phys. Rev. B 91, 241401(R) (2015)]

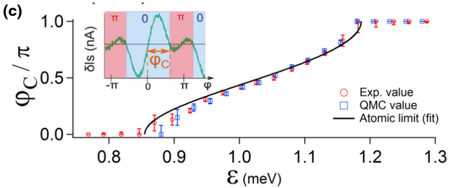

R. Delagrange et. al Phys. Rev. B 91, 241401(R) (2015)

- Experimental confirmation of the $0 - \pi$ transition controlled by the gate voltage in CNT by Delagrange et al.
- $\Delta = 0.17$meV and $U = 3.2$ meV were experimentally determined with the **uncertainty** $\sim 10\%$

Orsay experiment [Phys. Rev. B 91, 241401(R) (2015)]

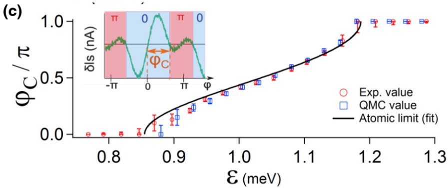

R. Delagrange et. al Phys. Rev. B 91, 241401(R) (2015)

- Experimental confirmation of the $0-\pi$ transition controlled by the gate voltage in CNT by Delagrange et al.
- $\Delta = 0.17$meV and $U = 3.2$ meV were experimentally determined with the **uncertainty** $\sim 10\%$
- The QMC calculations gave an excellent agreement for the shape and width of the $0-\pi$ boundary

Orsay experiment [Phys. Rev. B 91, 241401(R) (2015)]

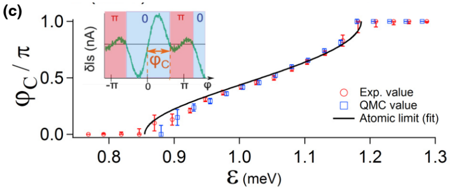

R. Delagrange et. al Phys. Rev. B 91, 241401(R) (2015)

- Experimental confirmation of the $0-\pi$ transition controlled by the gate voltage in CNT by Delagrange et al.
- $\Delta = 0.17$meV and $U = 3.2$ meV were experimentally determined with the **uncertainty** $\sim 10\%$
- The QMC calculations gave an excellent agreement for the shape and width of the $0-\pi$ boundary
- However, a **shift of the energy** level $\delta\varepsilon = 0.28$ meV was needed to overlap the experimental data

Orsay experiment [Phys. Rev. B 91, 241401(R) (2015)]

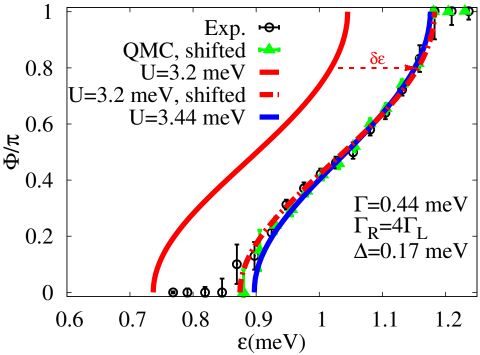

Orsay experiment [Phys. Rev. B 91, 241401(R) (2015)]

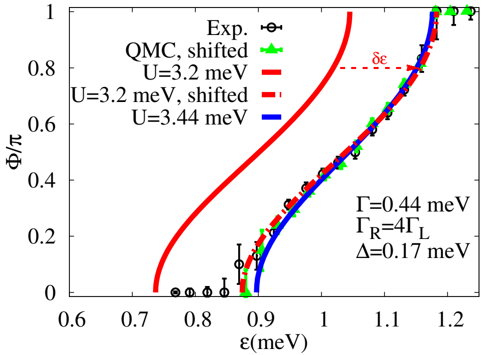

- We used the DC approximation and compared it with the experimental and QMC data

Orsay experiment [Phys. Rev. B 91, 241401(R) (2015)]

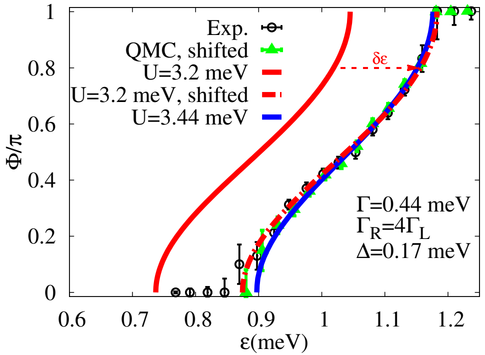

- We used the DC approximation and compared it with the experimental and QMC data
- We have reproduced the phase boundary almost perfectly with a small shift $\delta\varepsilon = 0.14$ meV

Orsay experiment [Phys. Rev. B 91, 241401(R) (2015)]

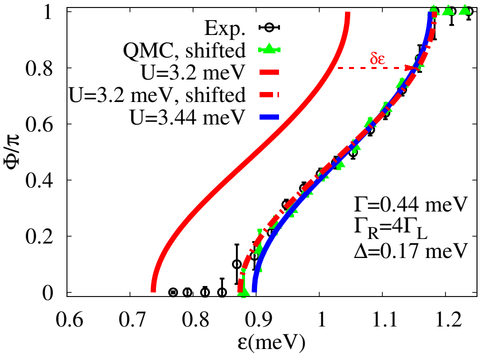

- We used the DC approximation and compared it with the experimental and QMC data
- We have reproduced the phase boundary almost perfectly with a small shift $\delta\varepsilon = 0.14$ meV
- We have checked how the boundary depends on the variance of used parameters.

Orsay experiment [Phys. Rev. B 91, 241401(R) (2015)]

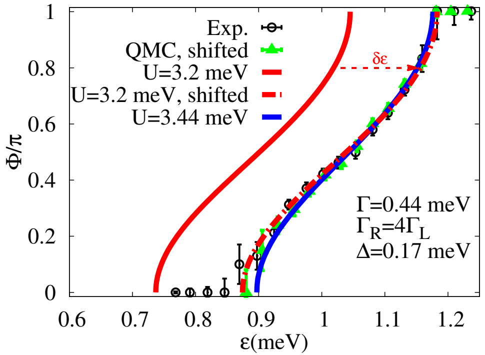

- We used the DC approximation and compared it with the experimental and QMC data
- We have reproduced the phase boundary almost perfectly with a small shift $\delta\varepsilon = 0.14$ meV
- We have checked how the boundary depends on the variance of used parameters.
- The shape and width of the boundary are robust within the 10% uncertainty

Orsay experiment [Phys. Rev. B 91, 241401(R) (2015)]

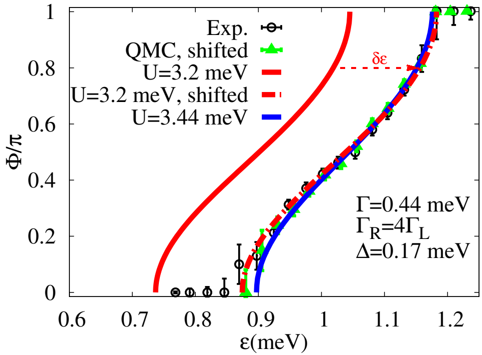

- We used the DC approximation and compared it with the experimental and QMC data
- We have reproduced the phase boundary almost perfectly with a small shift $\delta\varepsilon = 0.14$ meV
- We have checked how the boundary depends on the variance of used parameters.
- The shape and width of the boundary are robust within the 10% uncertainty
- The ε position of the boundary is very sensitive to the value of U

Orsay experiment [Phys. Rev. B 91, 241401(R) (2015)]

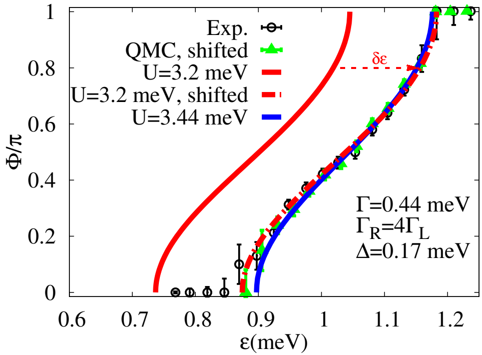

- **No shift** of the phase boundary is needed if $U = 3.44$ meV which is within the uncertainty of the experiment

- We used the DC approximation and compared it with the experimental and QMC data
- We have reproduced the phase boundary almost perfectly with a small shift $\delta\varepsilon = 0.14$ meV
- We have checked how the boundary depends on the variance of used parameters.
- The shape and width of the boundary are robust within the 10% uncertainty
- The ε position of the boundary is very sensitive to the value of U

Conclusions

- The self-consistent second-order perturbation expansion in the U of the superconducting SIAM can reliably substitute time and resources consuming numerical methods such us the NRG or QMC for a broad range of parameters

Conclusions

- The self-consistent second-order perturbation expansion in the U of the superconducting SIAM can reliably substitute time and resources consuming numerical methods such us the NRG or QMC for a broad range of parameters
- Its big potential was shown by analyzing two existing experimental data sets for the $0 - \pi$ phase boundary, including the suggestion for a plausible explanation of the existing discrepancy between the newest experiment and corresponding QMC results

Conclusions

- The self-consistent second-order perturbation expansion in the U of the superconducting SIAM can reliably substitute time and resources consuming numerical methods such us the NRG or QMC for a broad range of parameters
- Its big potential was shown by analyzing two existing experimental data sets for the $0 - \pi$ phase boundary, including the suggestion for a plausible explanation of the existing discrepancy between the newest experiment and corresponding QMC results
- **What next?**

Conclusions

- The self-consistent second-order perturbation expansion in the U of the superconducting SIAM can reliably substitute time and resources consuming numerical methods such us the NRG or QMC for a broad range of parameters
- Its big potential was shown by analyzing two existing experimental data sets for the $0 - \pi$ phase boundary, including the suggestion for a plausible explanation of the existing discrepancy between the newest experiment and corresponding QMC results
- **What next?**
- Extend the DC into π phase! Main problem is the **degenerate** doublet ground state (Guide: D.E. Logan et. al, PRB 90,075150 (2014)).

Conclusions

- The self-consistent second-order perturbation expansion in the U of the superconducting SIAM can reliably substitute time and resources consuming numerical methods such us the NRG or QMC for a broad range of parameters
- Its big potential was shown by analyzing two existing experimental data sets for the $0 - \pi$ phase boundary, including the suggestion for a plausible explanation of the existing discrepancy between the newest experiment and corresponding QMC results
- **What next?**
- Extend the DC into π phase! Main problem is the **degenerate** doublet ground state (Guide: D.E. Logan et. al, PRB 90,075150 (2014)).
- Three-terminal heterostructure arXiv:1609.08540:

Conclusions

- The self-consistent second-order perturbation expansion in the U of the superconducting SIAM can reliably substitute time and resources consuming numerical methods such us the NRG or QMC for a broad range of parameters
- Its big potential was shown by analyzing two existing experimental data sets for the $0 - \pi$ phase boundary, including the suggestion for a plausible explanation of the existing discrepancy between the newest experiment and corresponding QMC results
- **What next?**
- Extend the DC into π phase! Main problem is the **degenerate** doublet ground state (Guide: D.E. Logan et. al, PRB 90,075150 (2014)).
- Three-terminal heterostructure arXiv:1609.08540:

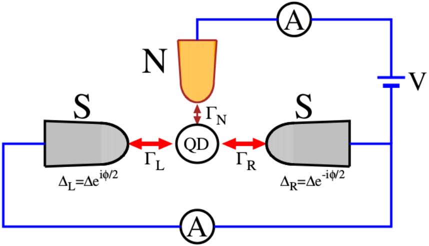

Thank you for your attention!

You can find more in our publications:

- M.Ž., V. Pokorný, V. Janiš and T. Novotný, *Phys. Rev. B* **93**, 024523 (2016)
- V. Janiš and V. Pokorný, M.Ž., *Eur. Phys. J. B* **89**, 197 (2016)
- M.Ž., V. Pokorný, V. Janiš and T. Novotný, *Sci. Rep.* **5**, 8821 (2015)
- V. Pokorný, V. Janiš, T. Novotný, M.Ž., *Acta Physica Polonica A* **126**, 352 (2014)

,